2011-06-08

Long-term corrosion resistance of iron-based amorphous metal coatings

Farmer, Joseph C.

Livermore, California. Lawrence Livermore National Laboratory

J. Farmer, T. Omlor, S. Menon, L. Brewer, (Long-term corrosion resistance of iron-based amorphous metal coatings," Department of Defense Corrosion

LAWRENCE
LIVERMORE
NATIONAL
LABORATORY

LLNL-CONF-485918

Long-Term Corrosion Resistance of Iron-Based Amorphous Metal Coatings

J. Farmer, T. Omlor, S. Menon, L. Brewer

June 8, 2011

Department of Defense Corrosion Conference 2011
Palm Springs, CA, United States
July 31, 2011 through August 5, 2011

Disclaimer

Long-Term Corrosion Resistance of Iron-Based Amorphous Metal Coatings

Joseph C. Farmer
Lawrence Livermore National Laboratory
7000 East Avenue
Livermore, CA 94550
United States of America

Timothy J. Omlor
Naval Postgraduate School
1 University Circle
Monterey CA 93943
United States of America

Sarath K. Menon
Naval Postgraduate School
1 University Circle
Monterey CA 93943
United States of America

Luke N. Brewer
Naval Postgraduate School
1 University Circle
Monterey CA 93943
United States of America

ABSTRACT

Novel iron-based amorphous metals, including SAM2X5 ($Fe_{49.7}Cr_{17.7}Mn_{1.9}Mo_{7.4}W_{1.6}B_{15.2}C_{3.8}Si_{2.4}$), SAM1651 ($Fe_{48.0}Cr_{15.0}Mo_{14.0}B_{6.0}C_{15.0}Y_{2.0}$), and other compositions have been developed for use as corrosion-resistant coatings for spent nuclear fuel containers, as criticality control materials, and as ultra-hard corrosion-resistant material for ship applications. These amorphous alloys appear to have corrosion resistance comparable to (or better than) that of Ni-based Alloy C-22 (UNS # N06022), based on measurements of breakdown potential and corrosion rate in seawater. A variety of characterization tools, including scanning electron microscopy, cyclic polarization, linear polarization and electrochemical impedance spectroscopy, have been used to develop a thorough understanding of the corrosion performance of these alloys over prolonged exposure in seawater and concentrated brines at elevated temperature.

Key words: high performance corrosion resistant materials, iron based amorphous metals, structural amorphous metals, SAM, SAM2X5, SAM1651, high velocity oxy fuel coating, HVOF, corrosion testing, salt fog, immersion testing, cyclic polarization, CP, linear polarization, LP, electrochemical impedance spectroscopy, EIS

INTRODUCTION

Novel iron-based amorphous metals, including SAM2X5 ($Fe_{49.7}Cr_{17.7}Mn_{1.9}Mo_{7.4}W_{1.6}B_{15.2}C_{3.8}Si_{2.4}$), SAM1651 ($Fe_{48.0}Cr_{15.0}Mo_{14.0}B_{6.0}C_{15.0}Y_{2.0}$), and other compositions have been developed for use as corrosion-resistant coatings for spent nuclear fuel containers, as criticality control materials, and as ultra-hard corrosion-resistant material for ship applications. These amorphous alloys appear to have corrosion resistance comparable to (or better than) that of Ni-based Alloy C-22 (UNS # N06022), based

on measurements of breakdown potential and corrosion rate in seawater. Chromium (Cr) and molybdenum (Mo) provide corrosion resistance, boron (B) enables glass formation, and rare earths such as yttrium (Y) lower critical cooling rate (CCR). SAM1651 has a nominal critical cooling rate of only 80 Kelvin per second due to the additions of yttrium, while SAM2X5 is characterized by relatively high critical cooling rates of approximately 600 Kelvin per second and has no yttrium. As previously reported, the hardness of Type 316L Stainless Steel is approximately 150 VHN, that of Alloy C-22 is approximately 250 VHN, and that of HVOF SAM2X5 ranges from 1100-1300 VHN. Such hardness makes these materials particularly attractive for applications where corrosion-erosion and wear are also issues. Since SAM2X5 has high boron content, it can absorb neutrons efficiently, and may therefore find useful applications as a criticality control material within the nuclear industry. A variety of characterization tools, including scanning electron microscopy, cyclic polarization, linear polarization and electrochemical impedance spectroscopy, have been used to develop a thorough understanding of the corrosion performance of these alloys over prolonged exposure in seawater and concentrated brines at elevated temperature.

The outstanding corrosion that may be possible with amorphous metals has been recognized for several years with a thorough discussion of their evolution previously published [1-11]. Compositions of several iron-based amorphous metals were published, including several with very good corrosion resistance. Examples included: thermally sprayed coatings of Fe-10Cr-10-Mo-(C,B), bulk Fe-Cr-Mo-C-B, and Fe-Cr-Mo-C-B-P. The corrosion resistance of an iron-based amorphous alloy with yttrium (Y), $Fe_{48}Mo_{14}Cr_{15}Y_2C_{15}B_6$ was also been established. Yttrium was added to this alloy to lower the critical cooling rate. Several nickel-based amorphous metals have been developed that exhibit exceptional corrosion performance in acids, but have not been included in this study, which is restricted to Fe-based materials. Very good thermal spray coatings of nickel-based crystalline coatings were deposited with thermal spray, but appear to have less corrosion resistance than nickel-based amorphous metals. Two iron-based amorphous metal coatings presented here as examples are SAM2X5 ($Fe_{49.7}Cr_{17.7}Mn_{1.9}Mo_{7.4}W_{1.6}B_{15.2}C_{3.8}Si_{2.4}$) and SAM1651 ($Fe_{48}Mo_{14}Cr_{15}Y_2C_{15}B_6$). These materials have been developed in the form of thin coatings, as well as thick layers forming composite surfaces, to provide exceptional corrosion resistance in environments including, but not limited to 5M $CaCl_2$ at 105-120°C and natural seawater at 30-90°C.

EXPERIMENTAL PROCEDURE

Samples of these coatings were produced by depositing corresponding amorphous metal powders on Ni-based Alloy C-22 substrates with a hydrogen-fueled high-velocity oxy-fuel (HVOF) process. In the case of linear polarization and corrosion potential measurements, the Alloy C-22 substrates were cylindrical rods, each having one hemispherical tip, with SAM2X5 deposited on the outer diameters of the rods, as well as over the entire surface of the hemispherical tip. The nominal length and diameter of each rod were 8 and 5/8 inches, respectively. The coating thickness was approximately 17 $\pm$ 2 mils.

Specific environments used for immersion testing of the SAM2X5 and SAM1651 HVOF coatings included: (1) natural seawater at 90°C; (2) 3.5-molal NaCl solution at 30°C; (3) 3.5-molal NaCl solution at 90°C; (4) 3.5-molal NaCl and 0.525-molal KNO_3 solution at 90°C; (5) simulated dilute water, referred to as SDW, at 90°C; (6) simulated concentrated water, referred to as SCW, at 90°C; and (7) simulated acidic water, referred to as SAW, at 90°C. Long-term corrosion testing was done with the standardized samples and electrochemical test stations like those shown in Figure 1.

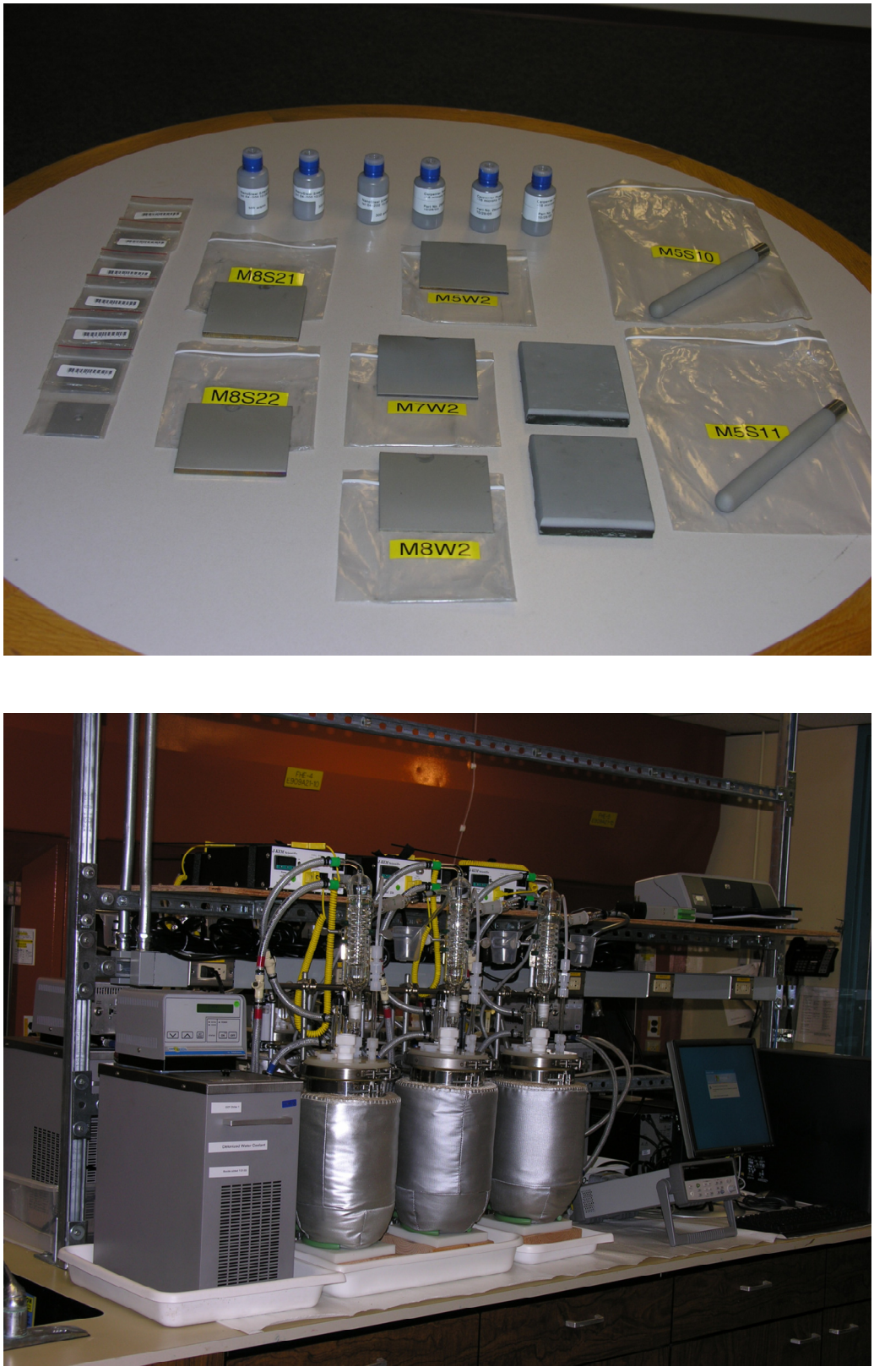

Figure 1: Samples of Standardized Iron-Based Amorphous-Metal HVOF Coatings Tested During Study (Upper Image) and Three Stations for Long-Term Corrosion Testing (Lower Image)

The linear polarization method was used as a method for determining the apparent corrosion rates of the various amorphous metal coatings. The procedure used for linear polarization testing consisted of the following steps: (1) holding the sample for ten seconds at the OCP; (2) beginning at a potential 20 mV below the OCP, increasing the potential linearly at a constant rate of 0.1667 mV per second to a potential 20 mV above the OCP; (3) recording the current being passed from the counter electrode to the working electrode as a function of potential relative to a standard Ag/AgCl reference electrode; and (4) determining the parameters in the cathodic Tafel line by performing linear regression on the voltage-current data, from 10 mV below the OCP, to 10 mV above the OCP. The slope of this line was the polarization resistance, *Rp* (ohms), and was defined in the published literature [12]. While no values for the Tafel parameter (*B*) of Fe-based amorphous metals have yet been developed, it was believed that a conservative value of approximately 25 mV was reasonable, based upon the range of published values for several Fe- and Ni-based alloys. The corrosion current density was then defined in terms of *B*, R_p and *A*, the actual exposed area of the sample being tested.

$$R_P = \left(\frac{\partial E}{\partial I} \right)_{E_{corr}} \qquad \textbf{(Equation 1)}$$

The parameter (*B*) was defined in terms of the slopes of the anodic and cathodic branches of the Tafel line:

$$B = \frac{\beta_a \beta_c}{2.303(\beta_a + \beta_c)} \qquad \textbf{(Equation 2)}$$

Values of B were published for a variety of iron-based alloys, and varied slightly from one alloy-environment combination to another. For example, values for carbon steel, as well as Type 304, 304L and 430 stainless steels, in a variety of electrolytes which include seawater, sodium chloride, and sulfuric acid, ranged from 19 to 25 mV. A value for nickel-based Alloy 600 in lithiated water at 288°C was given as approximately 24 mV. While no values have yet been developed for the Fe-based amorphous metals that are the subject of this investigation, it was believed that a conservative representative value of approximately 25 mV was appropriate for the conversion of polarization resistance to corrosion current. Given the value for Alloy 600, a value of 25 mV was also believed to be acceptable for converting the polarization resistance for nickel-based Alloy C-22 to corrosion current.

The general corrosion rate was calculated from the corrosion current density through application of Faraday's Law. The corrosion current, I_{corr} (A) was then defined as:

$$I_{corr} = \frac{B}{R_p} \qquad \textbf{(Equation 3)}$$

where the parameter B was conservatively assumed to be approximately 25 mV. The corrosion current density, i_{corr} (A cm^{-2}), was defined as the corrosion current, normalized by electrode area, *A* (cm^2). The corrosion (or penetration) rates of the amorphous alloy and reference materials were calculated from the corrosion current densities with the following formula:

$$\frac{dp}{dt} = \frac{i_{corr}}{\rho_{alloy} n_{alloy} F} \qquad \textbf{(Equation 4)}$$

where *p* was the penetration depth, *t* was time, i_{corr} was the corrosion current density, ρ_{alloy} was the density of the alloy (g cm^{-3}), n_{alloy} was the number of gram equivalents per gram of alloy, and *F* was Faraday's constant. The value of n_{alloy} was calculated with the following formula:

$$n_{alloy} = \sum_j \left(\frac{f_j n_j}{a_j} \right)$$ **(Equation 5)**

where f_j was the mass fraction of the j[th] alloying element in the material, n_j was the number of electrons involved in the anodic dissolution process, which was assumed to be congruent, and a_j was the atomic weight of the j[th] alloying element. Congruent oxidation or dissolution was assumed, which meant that the dissolution rate of a given alloy element was assumed to be proportional to its concentration in the bulk alloy. These equations were used to calculate factors for the conversion of corrosion current density to the corrosion rate. The conversion factors for converting corrosion current density to corrosion rate are approximately: 6.38 to 10.7 μm cm^2 μA^{-1} yr^{-1} for Type 316L stainless steel; 5.57 to 9.89 μm cm^2 μA^{-1} yr^{-1} for Alloy C-22; and 5.39 to 7.89 μm cm^2 μA^{-1} yr^{-1} for SAM2X5, depending upon the exact composition of each alloy within the specified ranges.

In addition to periodic in situ measurements of corrosion rate based upon the linear polarization method, it was also possible to use the potentiostat to perform electrochemical impedance spectroscopy (EIS), with the corrosion resistance of the two amorphous alloys in the various test environments over time reflected in the amplitude of the impedance measurements. During EIS the specimen produces a current response to an alternating potential signal. A small-amplitude sinusoidal voltage modulation (e) is applied between the reference and working electrode and a corresponding current response (i) flows between the counter and working electrodes [13-16]:

$$e = E \sin(\omega t))$$ **(Equation 6)**

$$i = I \sin(\omega t + \phi)$$ **(Equation 7)**

The voltage modulation (e) and current response (i) can also be represented in phasor notation as ($\dot{E}$) and ($\dot{I}$). The voltage modulation and current response are than related through the complex impedance (Z):

$$\dot{E} = \dot{I} Z$$ **(Equation 8)**

The complex impedance consists of real and imaginary parts, which are used to define the phase angle between the potential and current, as well as the magnitude of the impedance:

$$Z(\omega) = Z_r(\omega) + j Z_j(\omega)$$ **(Equation 9)**

The complex impedance, both its real and imaginary parts, is frequency dependent. From simple geometric arguments, the phase angle, the arctangent of the ratio of the imaginary to the real part of the complex impedance, can be determined:

$$\phi(\omega) = \arctan\left(\frac{Z_j(\omega)}{Z_r(\omega)} \right)$$ **(Equation 10)**

Similarly, the amplitude is defined as:

$$|Z(\omega)| = \sqrt{Z_r^2(\omega) + Z_j^2(\omega)}$$ **(Equation 11)**

Typically, materials resistant to corrosion in a particular environment, with corresponding good passivity, will exhibit a relatively high impedance amplitude at low frequency [16].

RESULTS

SAM2X5 HVOF coating samples were subjected to immersion testing. During these tests, linear polarization was used to determine the corrosion rate SAM2X5 HVOF coatings in the various test environments over period of approximately 135 days (the last linear polarization measurement made after 133 days). Following immersion testing and linear polarization measurements, samples were removed and photographed. This material experienced very little corrosion in SDW and SAW at 90°C, with slight corrosive attach in SCW at 90°C, as shown in Figure 2. The most severe attach was experienced in 3.5m NaCl solution at 90°C, with that corrosion mitigated by the addition of 0.525m KNO_3 inhibitor. These SAM2X5 samples performed reasonably well in heated seawater. The corresponding corrosion rates (microns per year) were determined from linear polarization measurements during the course of the test, and from weight loss and dimensional change at the end of the test. As shown in Figure 3, the corresponding corrosion rates based upon linear polarization after more than four months immersion were: (1) 12.3 μm/yr in natural seawater at 90°C; (2) 2.91 μm/yr in 3.5-molal NaCl solution at 30°C; (3) 176 μm/yr in 3.5-molal NaCl solution at 90°C; (4) 2.83 μm/yr in 3.5-molal NaCl and 0.525-molal KNO_3 solution at 90°C; (5) 2.61 μm/yr SDW at 90°C; (6) 12.4 μm/yr in SCW at 90°C; and (7) 81.1 μm/yr in SAW at 90°C.

A comparison of the electrochemical impedance spectra (EIS) for SAM2X5 HVOF samples in the aforementioned environments at the end of the immersion period are shown in Figure 4. As expected, the sample showing the most corrosive attack (SAM2X5 HVOF coating in 3.5m NaCl solution at 90°C) als0 gave the lowest impedance amplitude at low frequency (10 mHz). The sample in SDW remained pristine, and had the highest interfacial impedance at low frequency. Changes in EIS with time are shown in Figures 5, 6 and 7. In the case of EIS in 3.5m NaCl solution at 30°C (Figure 5), the low frequency impedance amplitude increased from 100 to 500 ohms over the duration of the test. In the case of EIS in NaCl at 90°C (Figure 6), the low frequency impedance amplitude increased from 20 to 70 ohms over the duration of the test. As expected, increased temperature decreased interfacial impedance and increased the corrosion rate. By adding 0.525m KNO_3 inhibitor to the 3.5m NaCl solution at 90°C, the interfacial impedance increased, and the corrosion rate decreased to the same levels measured without the inhibitor at 30°C (Figure 7).

After several years of additional materials development, optimized SAM1651 coatings were produced and subjected to immersion testing in the various test environments at 90°C. These coatings exhibited exceptional corrosion resistance in all environments, with some very sparse rust spots observed in near-boiling seawater {Figures 8 and 9). These spots have been attributed to ferrite particle impurities embedded in the amorphous metal coating during thermal spray operations. Examination of the coating cross-section with an environmental scanning electron microscope (ESEM) equipped with energy dispersive spectroscopy (EDS) showed that the spots were only superficial, with no through-coating corrosion (Figures 10 and 11). These spots may have been due to the corrosion of embedded particles of ferrite fed to the HVOF spray gun, which were virtually eliminated through process improvement and optimization.

The corrosion rate and corrosion potential of the optimized SAM1651 HVOF coating were monitored in situ during exposure for several months, and are graphically in Figures 12 through 13. As previously discussed, the linear polarization method was used to determine the corrosion rates shown in Figure 12. After 70 days, all corrosion rates were less than 10 micron per year, with rates in several cases less than 1 micron per year. Corresponding measurements of the open circuit corrosion potential are shown in Figure 13. The trend in OCP values towards more positive levels are believed to be due to slight changes in the passive film or surface composition during the test period. These tests show that the optimized SAM1651 HVOF coating has exceptional corrosion resistance, even after 4 months in concentrated brines at 90°C.mThe corrosion resistance of the amorphous metal coatings has also been verified during salt fog testing, and is discussed elsewhere [1-10].

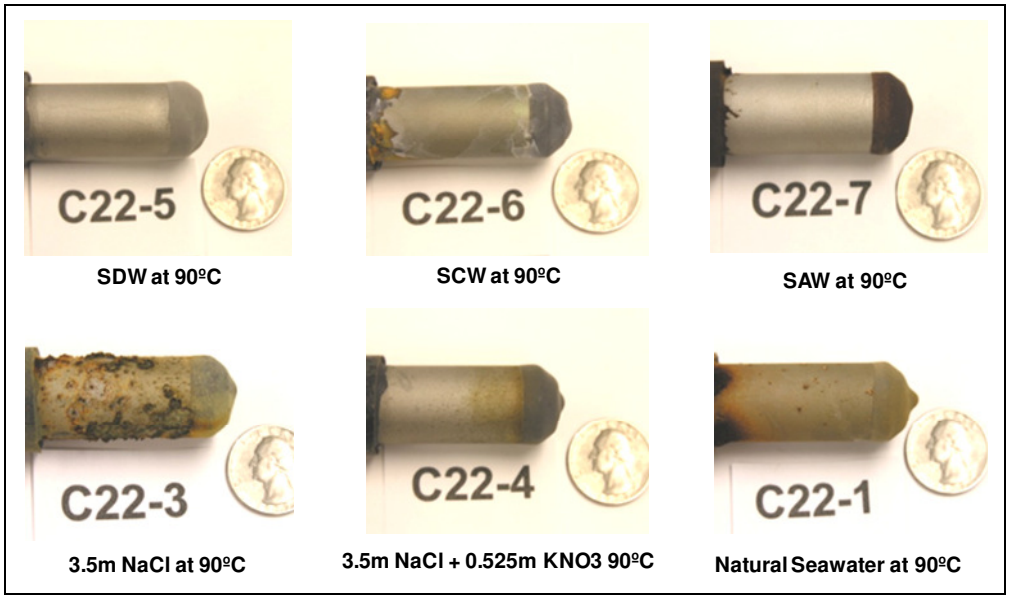

Figure 2: Corrosion of SAM2X5 HVOF Coatings Caused by Long Term Immersion Test

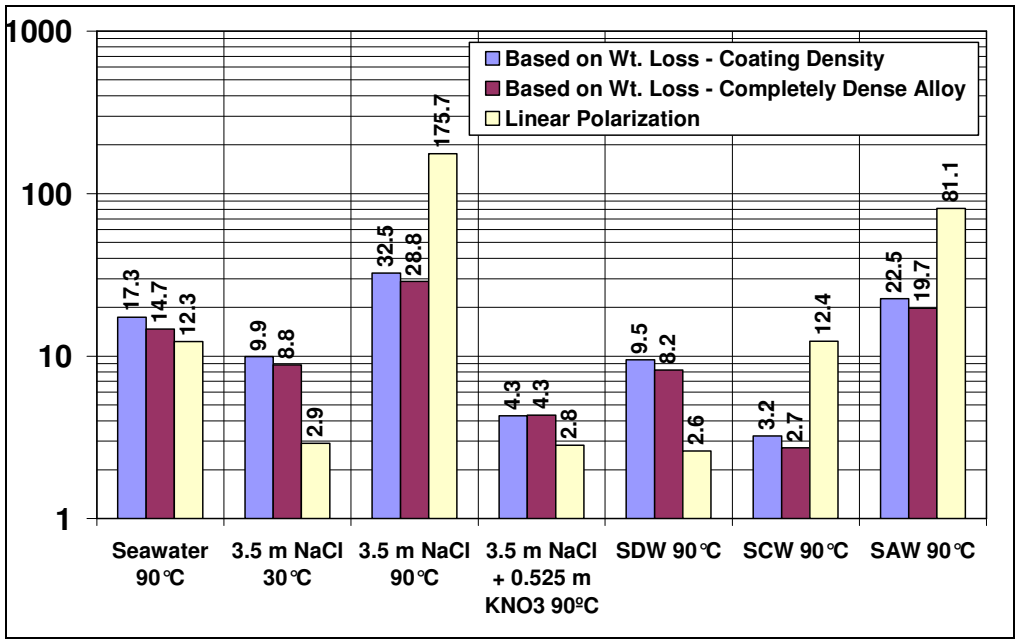

Figure 3: Corrosion Rates of SAM2X5 HVOF Coatings Measured During Immersion Testing for 135 Days – Given in Microns per Year

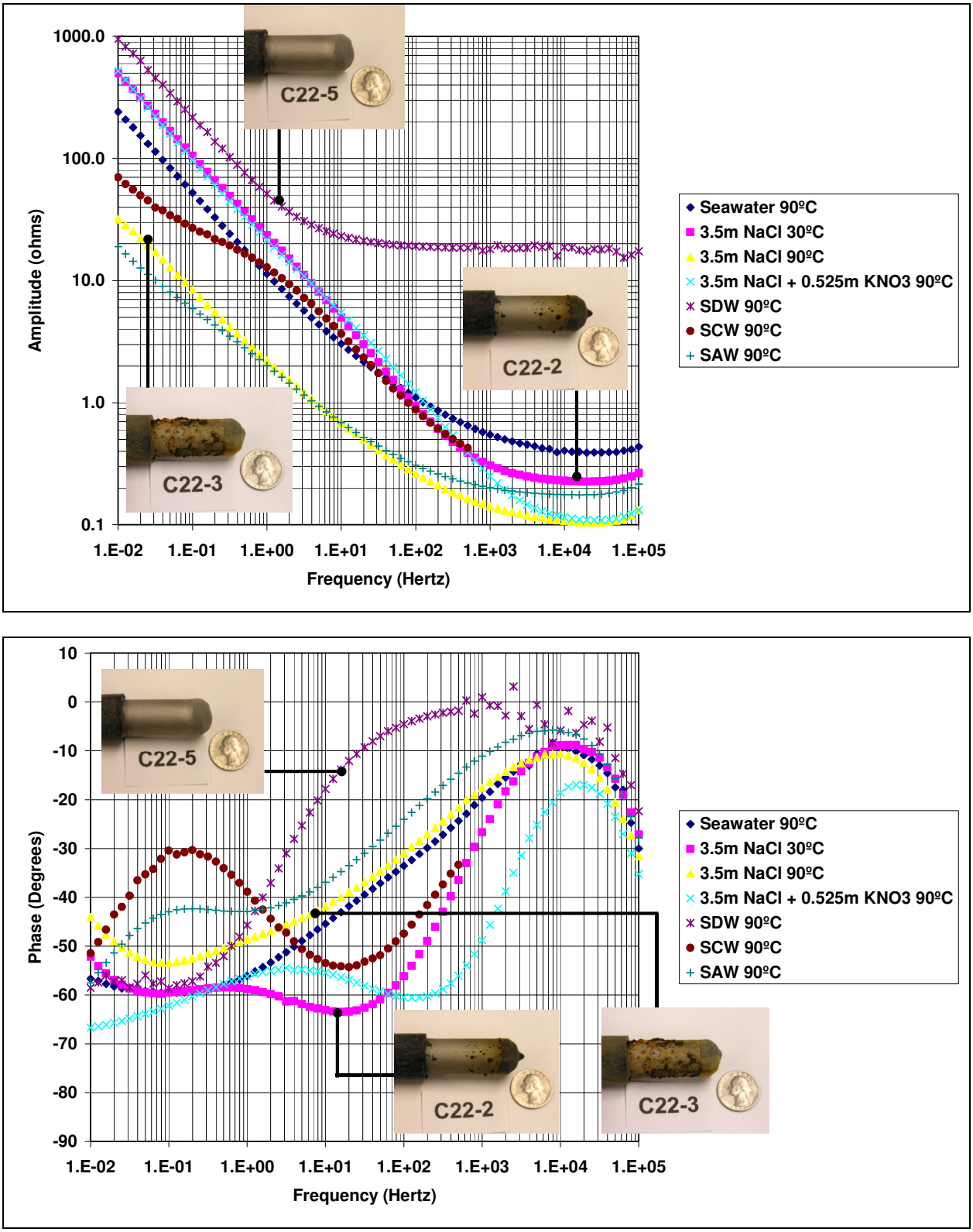

Figure 4: EIS of HVOF SAM2X5 (Lot #06-015) Response to Environments

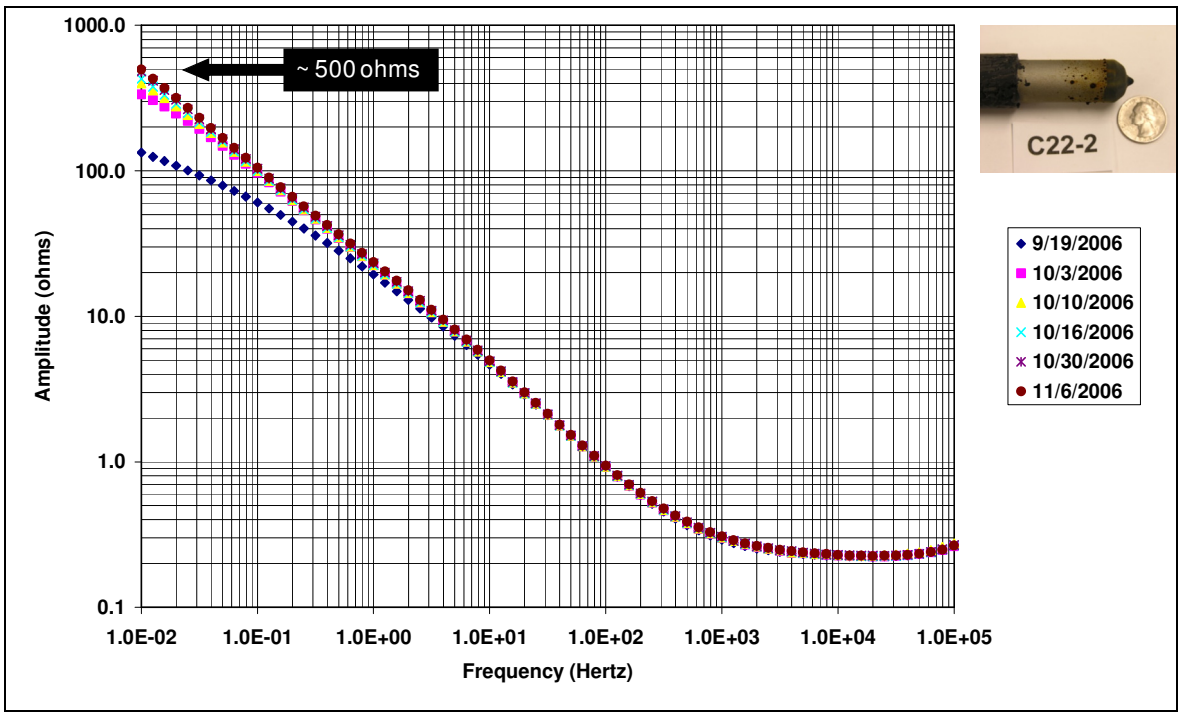

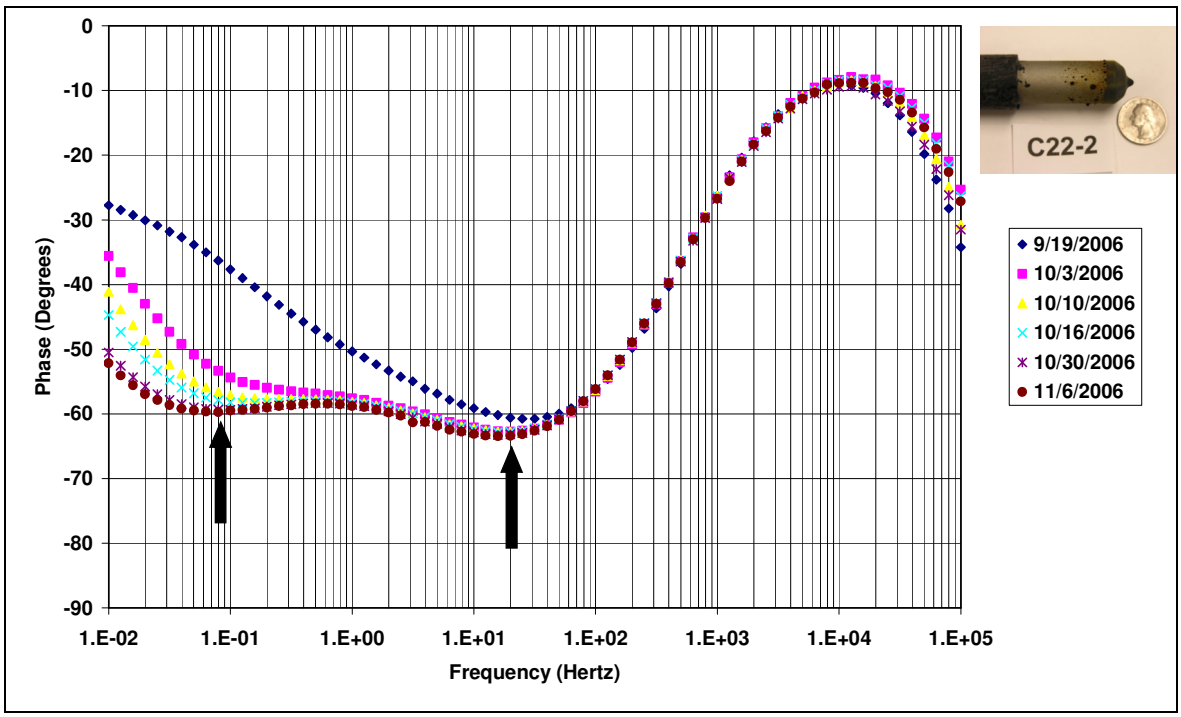

Figure 5: EIS of HVOF SAM2X5 (Lot #06-015) 3.5m NaCl 30°C

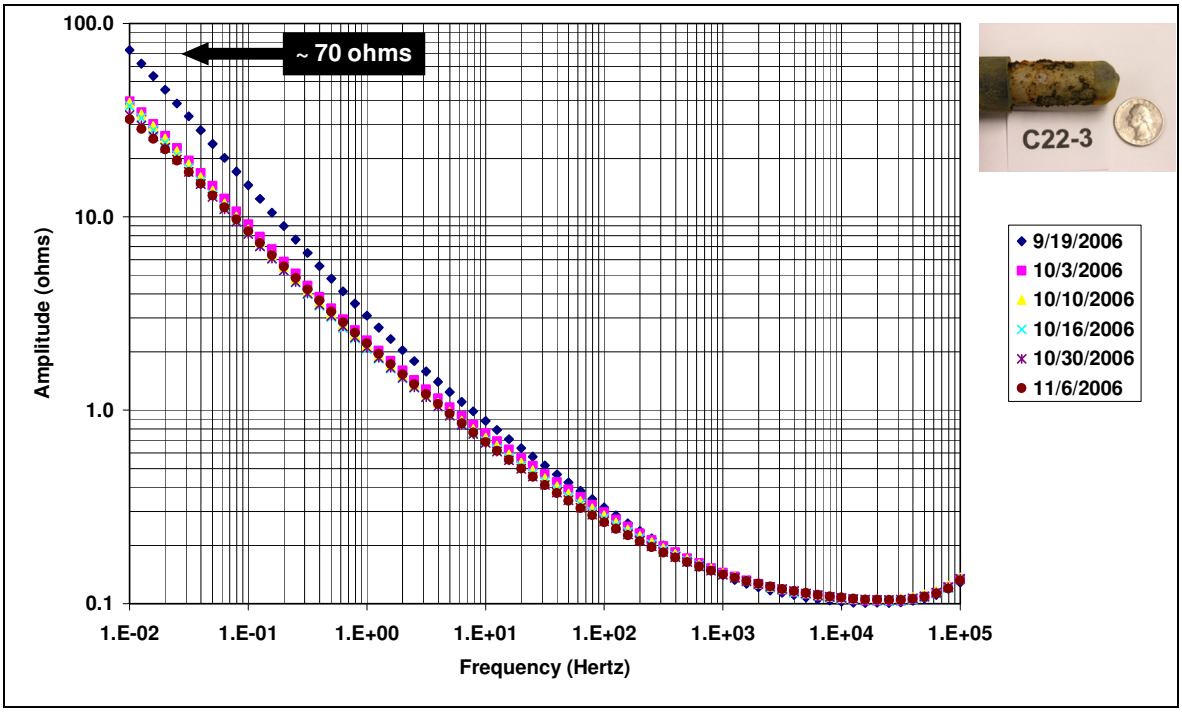

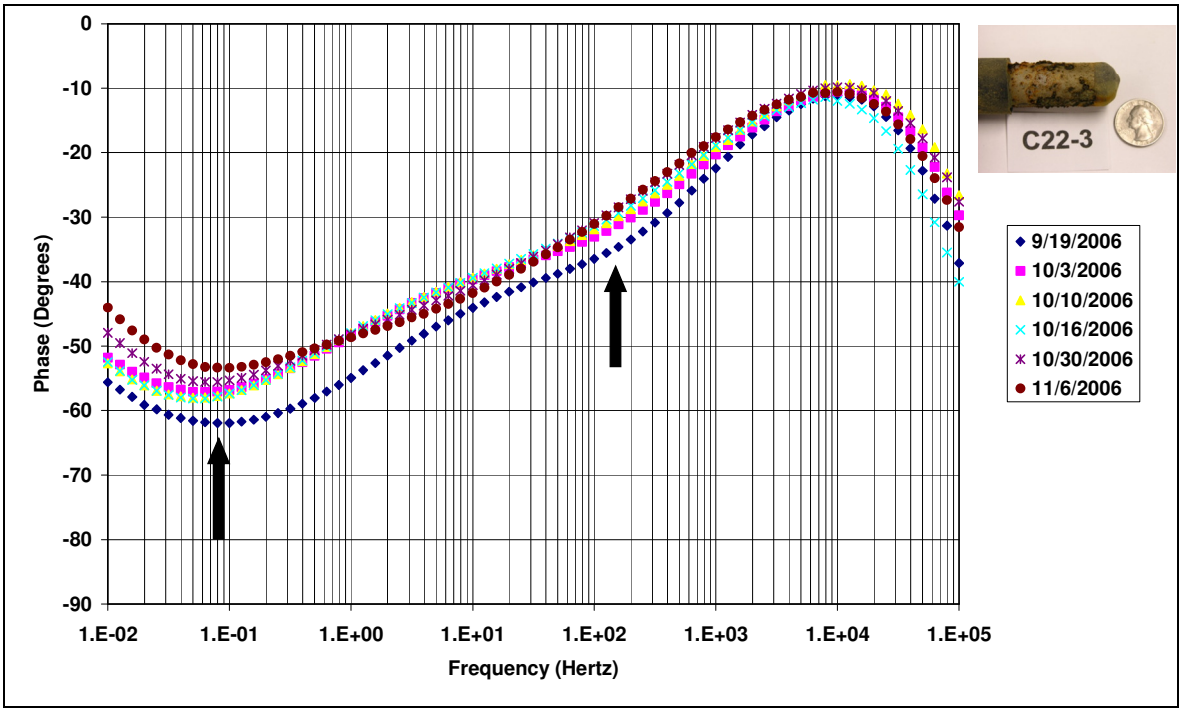

Figure 6: EIS of HVOF SAM2X5 (Lot #06-015) 3.5m NaCl 90°C

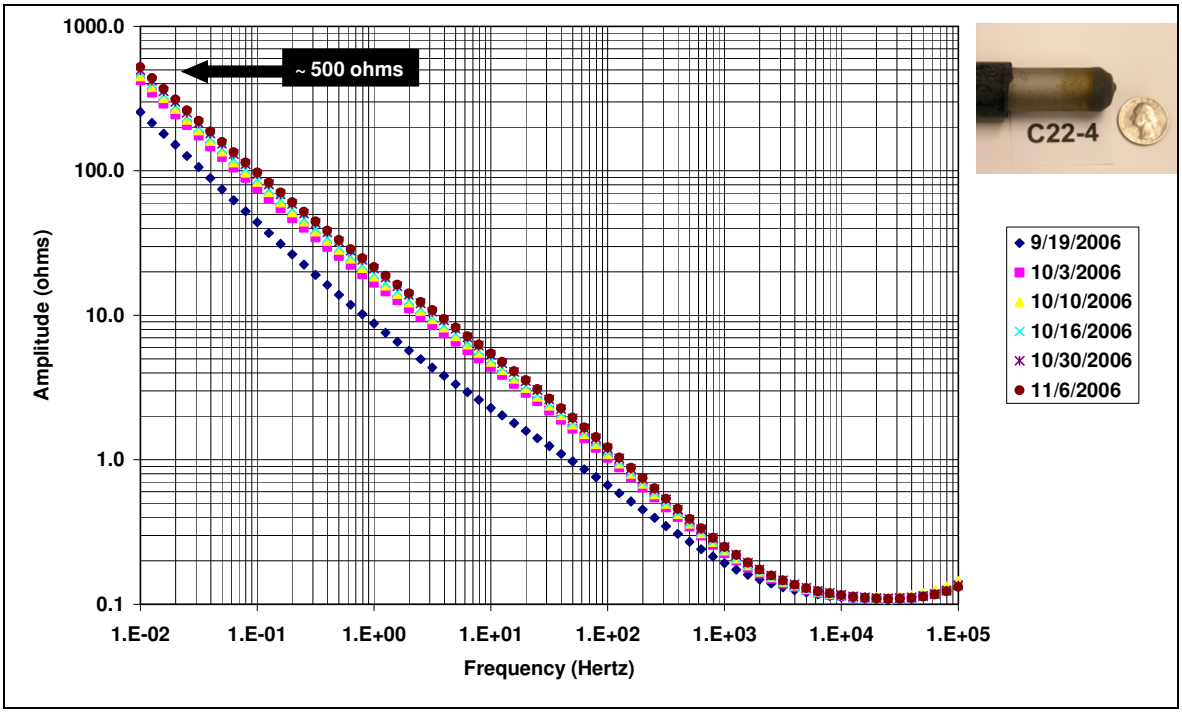

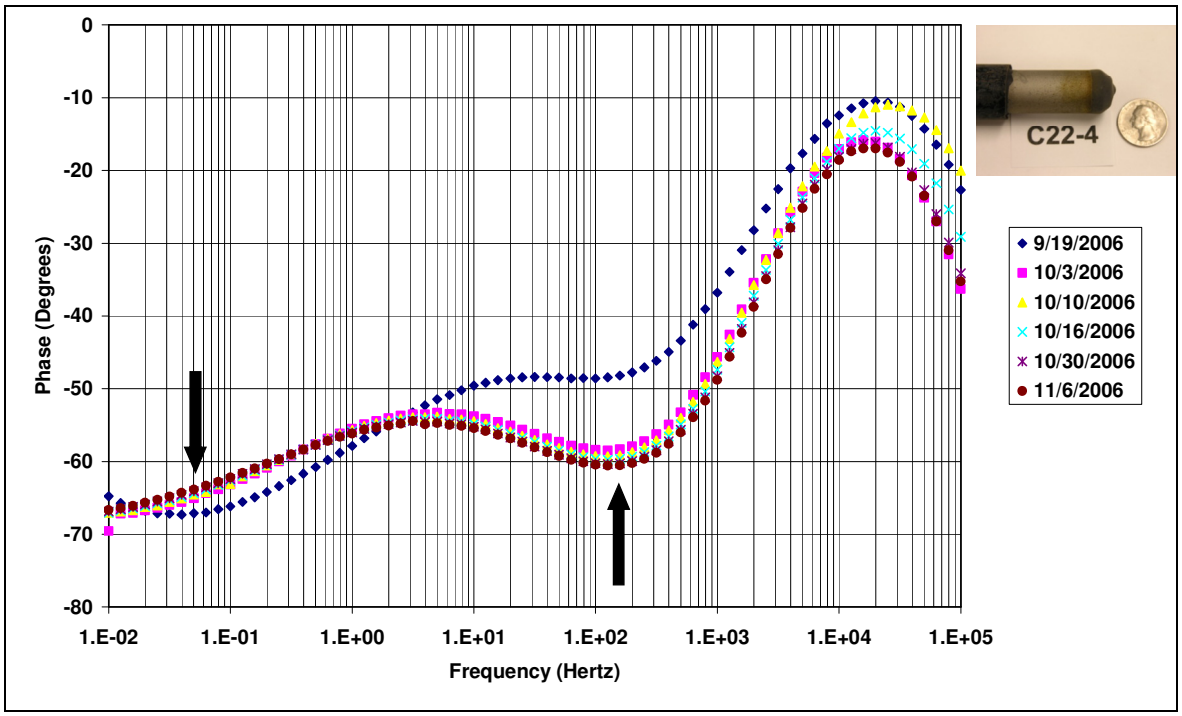

Figure 7: EIS of HVOF SAM2X5 (Lot #06-015) 3.5m NaCl + 0.525m KNO_3 90°C

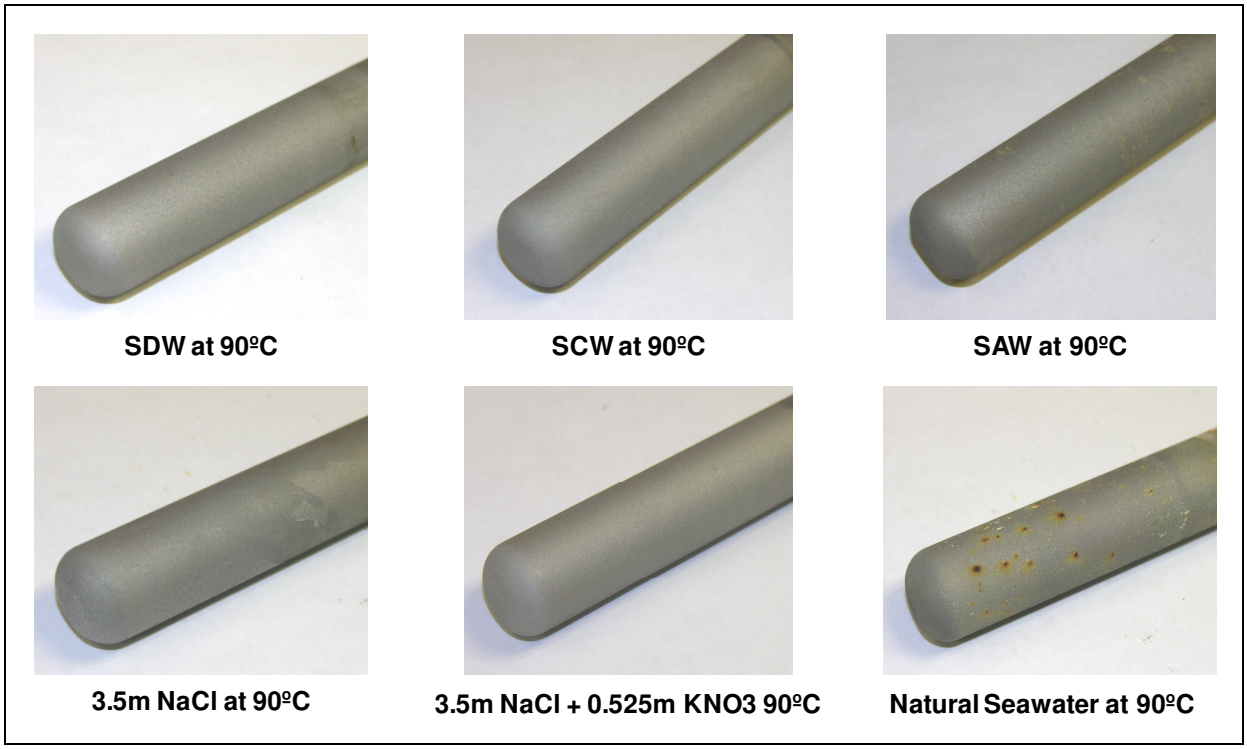

Figure 8: Optimized SAM1651 Coatings on OCP/LP/EIS Rods After 4 Months in Near-Boiling Concentrated Brines

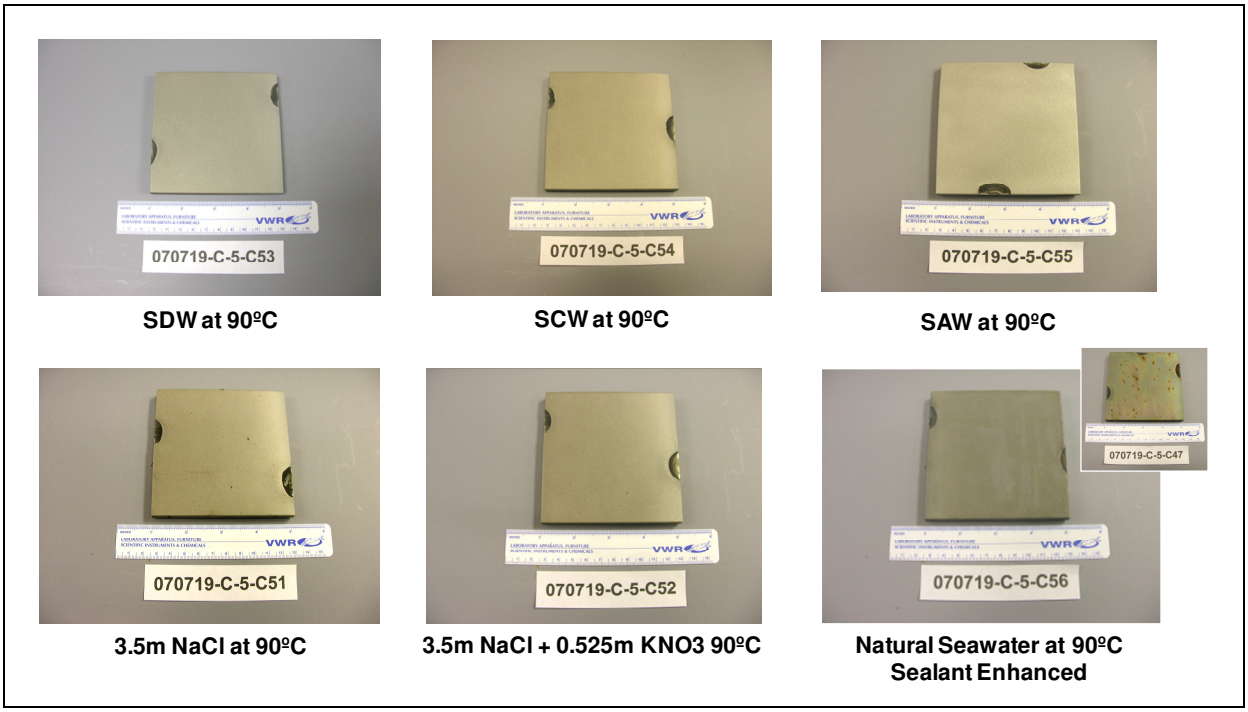

Figure 9: Optimized SAM1651 Coatings on 4-in x 4-in Plates After 4 Months in Near-Boiling Concentrated Brines

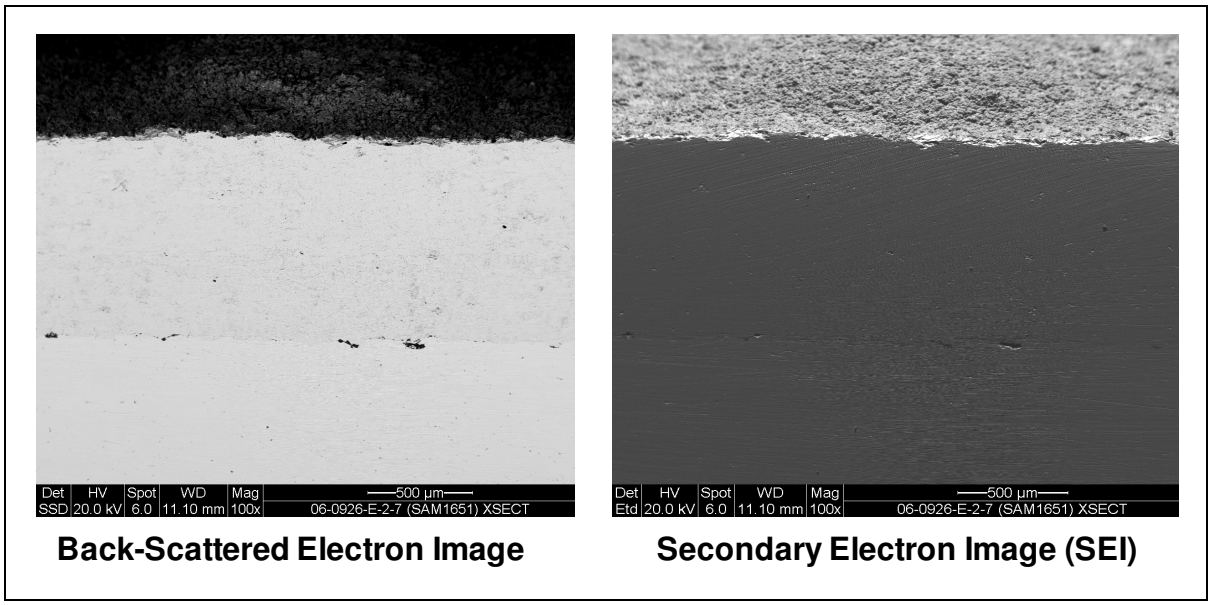

Figure 10: Un-Optimized SAM1651 Coating after Immersion for Four Months in 90°C Seawater: ESEM & EDS Characterization of Corrosion Spot Cross-Section

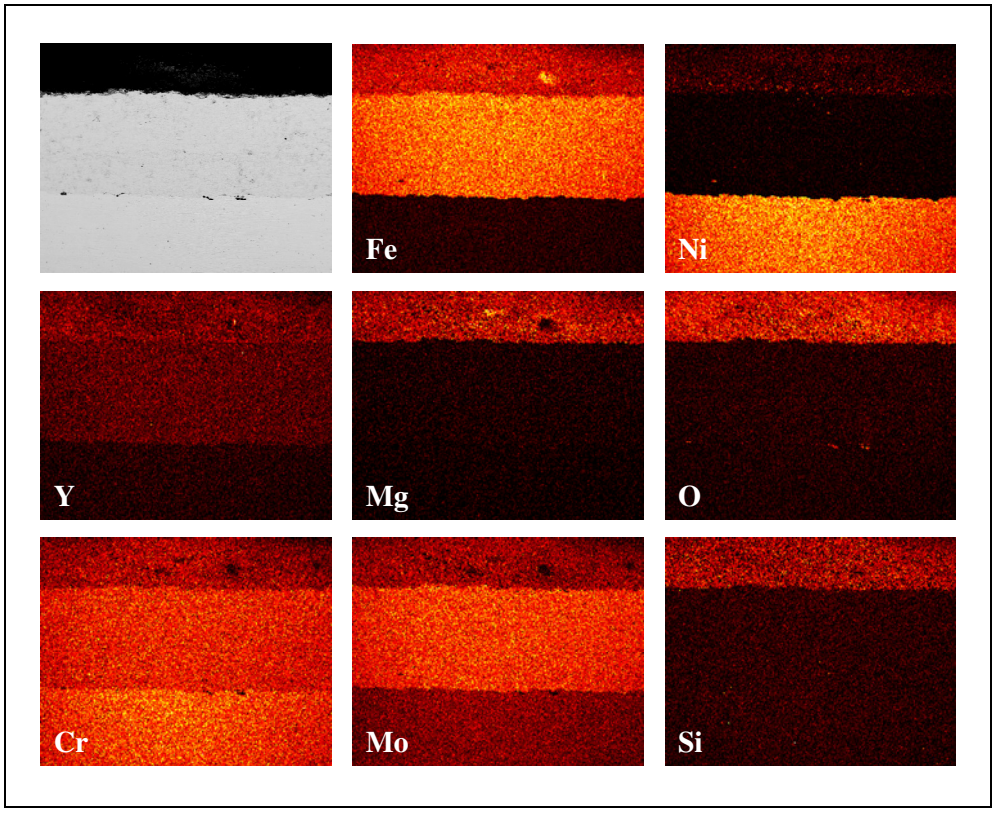

Figure 11: Mapping of Fe, Ni, Y, Mg, O, Cr, Mo and Si at Corrosion Site with Energy Dispersive Spectroscopy (EDS)

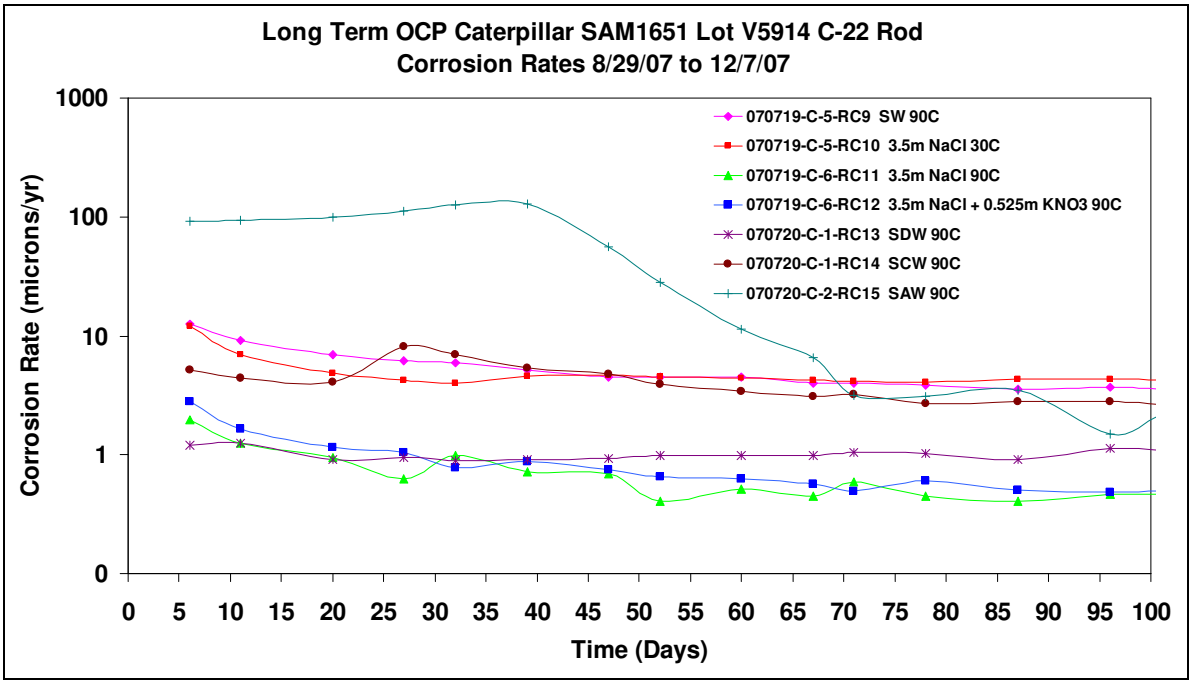

Figure 12: Optimized SAM1651 Coatings on Alloy C-22 Rods – Corrosion Rates Monitored *In Situ* with Linear Polarization Method for First 100 Days

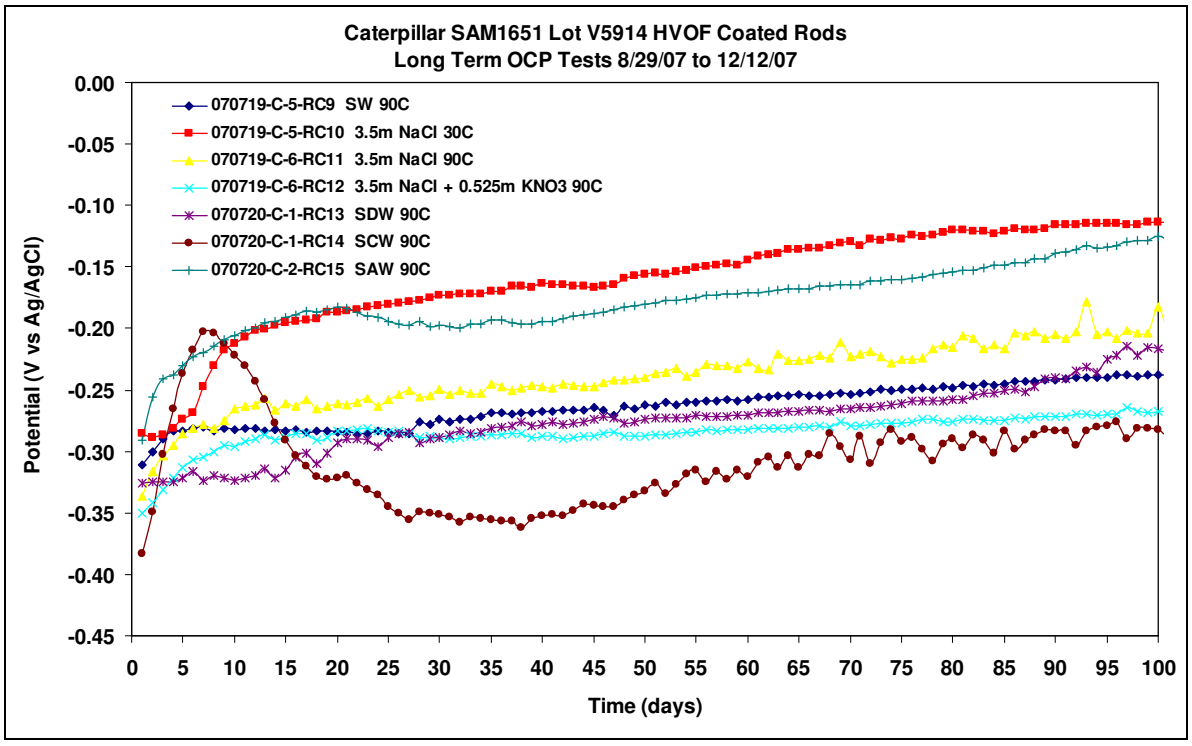

Figure 13: Optimized SAM1651 Coatings on Alloy C-22 Rods – Corrosion Potential Monitored *In Situ* for First 100 Days

CONCLUSIONS

Novel iron-based amorphous metals, including SAM2X5 ($Fe_{49.7}Cr_{17.7}Mn_{1.9}Mo_{7.4}W_{1.6}B_{15.2}C_{3.8}Si_{2.4}$), SAM1651 ($Fe_{48.0}Cr_{15.0}Mo_{14.0}B_{6.0}C_{15.0}Y_{2.0}$), and other compositions have been developed for use as corrosion-resistant coatings for spent nuclear fuel containers, as criticality control materials, and as ultra-hard corrosion-resistant material for ship applications. These amorphous alloys appear to have corrosion resistance comparable to (or better than) that of Ni-based Alloy C-22 (UNS # N06022), based on measurements of breakdown potential and corrosion rate in seawater. Long term immersion tests were conducted with these materials. Corrosion rates were determined throughout the test with linear polarization, while electrochemical impedance spectroscopy was used to gain additional insight into the integrity of the passive film. SAM1651 exhibited better passivity and lower corrosion rates than the SAM2X5 in the test environments explored during this study.

ACKNOWLEDGEMENTS

Lawrence Livermore National Laboratory (LLNL) is operated by Lawrence Livermore National Security, LLC, for the U.S. Department of Energy, National Nuclear Security Administration under Contract DE-AC52-07NA27344. The enabling support of LLNL is greatly appreciated. Karl van Bibber, Vice President of Research, Knox Millsaps, Professor and Chairman of Mechanical and Aerospace Engineering, and Terry McNelley, Distinguished Professor of Mechanical and Aerospace Engineering, are gratefully acknowledged for their role making this collaborative work possible.

REFERENCES

1. J. Farmer, P. Turchi, J. Perepezko, Iron-Based Amorphous Metals, An Important Family of High-Performance Corrosion-Resistant Materials, Metallurgical and Materials Transactions A 40A, 6 (2009) pp. 1288.
2. J. Farmer, J-S. Choi C-K. Saw, J. Haslam, D. Day, P. Hailey, T. Lian, R. Rebak, J. Perepezko, J. Payer, D. Branagan, M. Beardsley, A. D'Amato, L Aprigliano, Iron-Based Amorphous Metals: High-Performance Corrosion-Resistant Material Development, Metallurgical and Materials Transactions A, 40A, 6 (2009) pp. 1289-1305.
3. J. Blink, J. Farmer, J-S. Choi, C-K. Saw, Applications in the Nuclear Industry for Thermal Spray Amorphous Metal and Ceramic Coatings, Metallurgical and Materials Transactions A, 40A, 6 (2009) pp. 1345-1354.
4. Larry Kaufman, J. H. Perepezko, K. Hildal, J. Farmer, D. Day, N. Yang, D. Branagan, Transformation, stability and Pourbaix Diagrams of High Performance Corrosion Resistant (HPCRM) Alloys, Computer Coupling of Phase Disgrams and Thermochemistry, CALPHAD Journal, 33, 1 (2009) 11 p. (doi:10.1016/j.calphad.2008.09.0919) (www.elsevier.com/locate/calphad).
5. J. C. Farmer, J-S. Choi, C-K. Saw, R. H. Rebak, S. D. Day, T. Lian, P. D. Hailey, J. H. Payer, D. J. Branagan and L. F. Aprigliano, Corrosion Resistance of Amorphous $Fe_{49.7}Cr_{17.7}Mn_{1.9}Mo_{7.4}W_{1.6}B_{15.2}C_{3.8}Si_{2.4}$ Coating – A New Criticality Control Material, Journal of Nuclear Technology, 161, 2 (2008) pp. 169-189.

6. R. B. Rebak, S. D. Day, T. Lian, P. D. Hailey, J. C. Farmer, Environmental Testing of Iron-Based Amorphous Alloys, Metallurgical and Materials Transactions A, 39A, 2 (2008) pp. 225-234 (doi: 10.1007/s11661-007-9460-7).
7. J. C. Farmer, J. J. Haslam, S. D. Day, T. Lian, C. K. Saw, P. D. Hailey, J-S. Choi, R. B. Rebak, N. Yang, J. H. Payer, J. H. Perepezko, K. Hildal, E. J. Lavernia, L. Ajdelsztajn, D. J. Branagan, L. F. Aprigliano, Corrosion Resistance of Thermally Sprayed High-Boron Iron-Based Amorphous-Metal Coatings: $Fe_{49.7}Cr_{17.7}Mn_{1.9}Mo_{7.4}W_{1.6}B_{15.2}C_{3.8}Si_{2.4}$, Journal of Materials Research, 22, 8 (2007) pp. 2297-2311.
8. Olivia A. Graeve, Raghunath Kanakala, Larry Kaufman, Kaustav Sinha, Enhai Wang, Brett Pearson and Joseph C. Farmer, Spark Plasma Sintering of Fe-Based Structural Amorphous Metals (SAM) with Y_2O_3 Nanoparticle Additions, Materials Letters (2007) (doi:10.1016/j.matlet.2008.01.092/4 p.).
9. J. C. Farmer, Frank M. G. Wong, Jeffery, J. Haslam, Nany Yang, Enrique J. Lavernia, Craig A. B.ue, Olivia A. Graeve, Robert Bayles, John H. Perepezko, Larry Kaufman, Julie Schoenung, Leo Ajdelsztajn, Corrosion Resistant Amorphous Metals and Methods of Forming Corrosion Resistant Amorphous Metals, U. S. Pat. No. 7,618,500 B2 (November 17, 2009).
10. D. Branagan, Method of Modifying Iron-Based Glasses to Increase Crystallization Temperature Without Changing Melting Temperature, U.S. Pat. Appl. No. 20040250929, Filed Dec. 16, 2004.
11. D. Branagan, Properties of Amorphous/Partially Crystalline Coatings (U.S. Pat. Appl. No. 20040253381, Filed Dec. 16, 2004).
12. R.S. Treseder, R. Baboian and C. G. Munger, Polarization Resistance Method for Determining Corrosion Rates, NACE Corrosion Engineer's Reference Book (Second Edition, National Association of Corrosion Engineers, 1440 South Creek Drive, Houston, Texas, 2992) pp. 65-66, 156, 180.
13. A.J. Bard, L.R. Faulkner, *Electrochemical Methods, Fundamentals and Applications* (John Wiley & Sons, New York, NY, 1980).
14. H. Shih, *Electrochemical Impedance Spectroscopy (EIS), Technology and Applications* (The Electrochemical Society, Pennington, NJ, 2006).
15. M.E. Orazem, *General Electrochemistry and Introduction to Impedance Spectroscopy, Motivation, Representation of Impedance Date, Impedance Measurement, and Discussion* (The Electrochemical Society, Pennington, NJ, 2005).
16. J.C. Farmer, S. Menon, P. Legrand, "Effect of FSP on the Electrochemical Activity and Passive Film Stability of Ni-Al Bronze" (Extended Abstracts, 219th Meeting of the Electrochemical Society Meeting, Montreal, Canada, May 2011).